JOURNAL OF AIRCRAFT
Vol. 46, No. 2, March–April 2009

Optimization of Flapping Motion Parameters for Two Airfoils in a Biplane Configuration

Mustafa Kaya* and Ismail H. Tuncer†
Middle East Technical University, 06531 Ankara, Turkey
and
Kevin D. Jones‡ and Max F. Platzer§
Naval Postgraduate School, Monterey, California 93943

DOI: 10.2514/1.38796

Flapping motion parameters of airfoils in a biplane configuration are optimized for maximum thrust and/or propulsive efficiency. Unsteady, viscous flowfields over airfoils flapping in a combined plunge and pitch are computed with a parallel flow solver on moving and deforming overset grids. The amplitudes of the sinusoidal pitch and plunge motions and the phase shift between them are optimized for a range of flapping frequencies. A gradient-based optimization algorithm is implemented in a parallel computing environment. The deforming overset grids employed remove the restriction on the flapping motion of airfoils, and improve the optimization results obtained earlier. In the Strouhal number range $0.17 < Sr < 0.25$, an airfoil in a biplane configuration produces more thrust than a single airfoil. Yet, at a higher Strouhal number, the airfoil in a biplane configuration produced less thrust at a significantly lower efficiency than a single flapping airfoil.

Nomenclature

C_d = drag coefficient
C_p = pressure coefficient
C_P = power coefficient
C_t = average thrust coefficient
c = airfoil chord length
h = plunge position
h_0 = plunge amplitude
k = reduced frequency, $\omega c/U_\infty$
M = freestream Mach number
Re = Reynolds number based on the chord length
Sr = Strouhal number
T = period of a flapping motion
t = time
U_∞ = freestream velocity
$\mathbf{V}$ = velocity vector
y_0 = mean distance between the airfoils
α = pitch angle
α_0 = pitch amplitude
β = weight of the efficiency in the objective function
η = propulsive efficiency
ϕ = phase shift between plunge and pitch motions
ω = angular frequency

I. Introduction

BASED on observations of flying birds, insects, and swimming fish, it appears that flapping wings may be advantageous for flights of very small-scale vehicles, so-called micro air vehicles (MAVs), with wingspans of 15 cm or less. The current interest in the research and development community is to find the most energy-efficient airfoil adaptation and flapping wing motion technologies capable of providing the required aerodynamic performance for MAV flight.

Recent experimental and computational studies investigated the kinematics, dynamics, and flow characteristics of flapping wings, and shed some light on the lift, drag, and propulsive power considerations [1,2]. In their experimental study, Lai and Platzer [3] investigate drag-producing wake flows and thrust-producing jetlike flows downstream of a plunging airfoil. Water-tunnel flow visualization experiments by Jones et al. [4] provide a considerable amount of information on the wake characteristics of flapping airfoils. In their experiments, Anderson et al. [5] observe that the phase shift between pitch and plunge oscillations plays a significant role in maximizing the propulsive efficiency. A recent experimental study by Schouveiler et al. [6] shows that high thrust and efficiency conditions can both be achieved for some range of flapping parameters.

Lewin and Haj-Hariri [7] examine the propulsive characteristics of an airfoil plunging over a range of frequencies and plunge amplitudes to correlate viscous flow structures to thrust generation. Hover et al. [8] use different effective angle-of-attack variations in time to investigate the propulsive performance of an airfoil undergoing combined plunge and pitch oscillations. Lee et al. [9] identify the key physical flow phenomenon dictating the thrust generation of a plunging and/or pitching airfoil in terms of flow and/or geometry parameters.

Navier–Stokes computations performed by Tuncer and Platzer [10] show that an airfoil undergoing combined pitch and plunge oscillations may produce high thrust at a high propulsive efficiency under certain kinematic conditions. Tuncer et al. [11,12] also observe that the thrust and the propulsive efficiency values may be significantly increased in the case of flapping/stationary airfoil combinations in tandem. Using a Navier–Stokes solver, Isogai et al. [13] explore the effect of dynamic stall phenomena on the thrust generation and the propulsive efficiency of flapping airfoils. Young and Lai [14] show that the vortical wake structures and the lift and thrust characteristics of a plunging airfoil are strongly dependent on the oscillation frequency and amplitude.

Jones et al. [15] recently demonstrated a radiocontrolled micro air vehicle propelled by flapping wings in a biplane configuration (Fig. 1). The experimental and numerical studies by Jones et al. [16–18] and Platzer and Jones [19] on flapping-wing propellers points at

Presented as Paper 0420 at the 45th AIAA Aerospace Sciences Meeting and Exhibit, Reno, NV, 8–11 January 2007; received 28 May 2008; accepted for publication 14 November 2008.

*Graduate Student, Department of Aerospace Engineering.
†Professor, Department of Aerospace Engineering. Member AIAA.
‡Research Associate Professor, Department of Mechanical and Astronautical Engineering. Senior Member AIAA.
§Professor Emeritus in Department of Mechanical and Astronautical Engineering. Fellow AIAA.

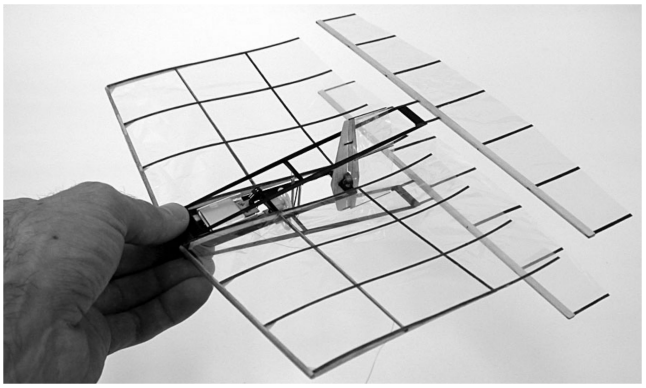

Fig. 1 Flapping-wing MAV model.

the gap between numerical flow solutions and the actual flight conditions over flapping wings.

Tuncer and Kaya [20–22] investigated the optimization of flapping motion parameters for maximizing thrust and propulsive efficiency of flapping airfoils. In the study [20] with a biplane configuration (Fig. 2), the moving overset grid system (Fig. 3), which did not allow airfoil grids to overlap onto each other, imposed restrictions on the plunge and pitch amplitudes. In the present study, the moving overset grid system is enhanced with the addition of a grid deformation capability, as shown in Fig. 3.

In this study, the sinusoidal motion parameters of two flapping airfoils in a biplane configuration are optimized for maximum thrust and/or propulsive efficiency using a gradient-based optimization algorithm. The optimization algorithm and the unsteady flow solutions on moving/deforming overset grids are obtained in a parallel computing environment. The optimum flapping motions and the unsteady flowfields are then analyzed for distinguishing features.

II. Numerical Method

Two-dimensional unsteady viscous flows around flapping airfoils in a biplane configuration are computed by solving the Navier–Stokes equations on moving and deforming overset grids. A domain-decomposition-based parallel computing algorithm is employed. Parallel Virtual Machine (PVM) message passing library routines are used in the parallel solution algorithm. A gradient-based optimization is employed for the optimization of flapping motion parameters. The computed unsteady flowfields are analyzed in terms of time histories of aerodynamic loads and unsteady particle traces.

A. Navier–Stokes Solver

The strong conservation-law form of the 2-D Navier–Stokes equations is solved implicitly on overset grids. The convective fluxes are evaluated using the third-order accurate Osher's upwind biased flux difference splitting scheme. The discretized equations are solved by an approximately factored, implicit algorithm [10,12]. At the overlapping subgrid boundaries of the overset grid system, the conservative flow variables are exchanged/interpolated among the subgrids at every time step.

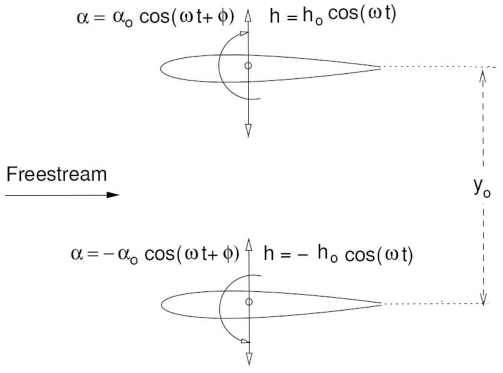

Fig. 2 Out-of-phase flapping motion of two airfoils in a biplane configuration.

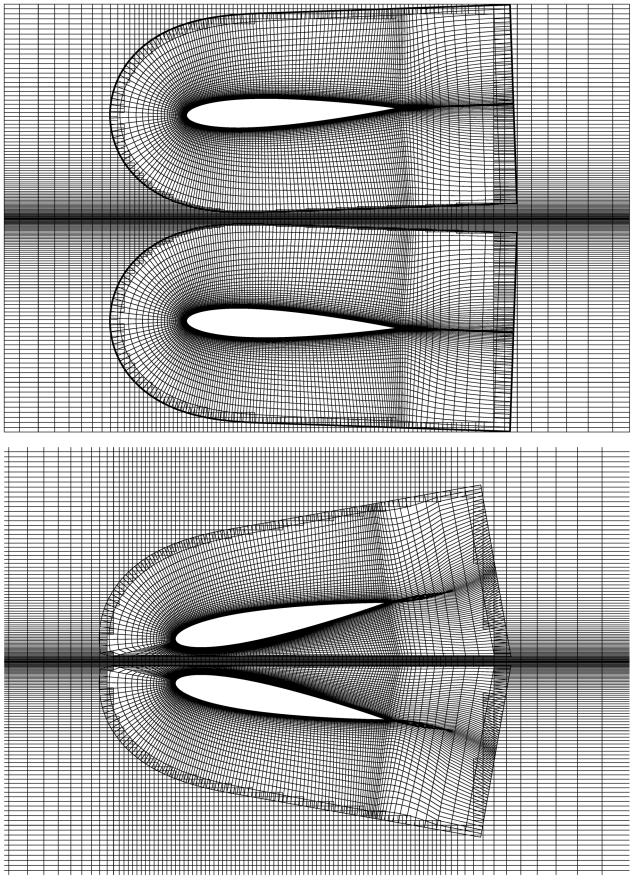

Fig. 3 Moving and moving-deforming overset grid system.

The out-of-phase flapping motion of the airfoils in biplane configuration is imposed by moving the airfoils and the C-type grids around them over the background grid (Fig. 3). The airfoil grids are deformed as they come close to the symmetry line between the airfoils. The flapping motion of the upper airfoil in a combined plunge and pitch is described by

$$h = -h_0 \cos(\omega t) \tag{1}$$

$$\alpha = -\alpha_0 \cos(\omega t + \phi) \tag{2}$$

The pitch axis is located at the midchord. The flapping motion of the lower airfoil is in counterphase. The grid velocities are computed analytically in the pure grid movement regions. In moving and deforming grid regions, a first-order finite difference expression is used.

B. Effective Angle of Attack

An important parameter for analyzing the performance of the flapping airfoils is the instantaneous effective angle of attack. The effective angle of attack due to the pitching and plunging velocities at the leading edge is defined by

$$\alpha_{\text{eff}}(t) = \alpha(t) - \arctan\left(\frac{\dot{h}(t) + \frac{1}{2}c\dot{\alpha}(t)\cos(\alpha(t))}{U_\infty - \frac{1}{2}c\dot{\alpha}(t)\sin(\alpha(t))}\right) \tag{3}$$

where $\frac{1}{2}c$ is the distance between the leading edge and the pitch axis.

C. Optimization

The objective function is taken as a linear combination of the average thrust coefficient C_t and the propulsive efficiency η over a

flapping period:

$$O[C_t, \eta] = (1-\beta)\frac{C_t^n}{C_t^{n-1}} + \beta\frac{\eta^n}{\eta^{n-1}} \tag{4}$$

where n denotes the optimization step.

The thrust coefficient is based on the integration of the drag coefficient over a flapping period. The propulsive efficiency is the ratio of the power extracted through thrust to the power input required to sustain the flapping motion:

$$C_t = \frac{1}{T}\int_t^{t+T} C_d \, \mathrm{d}t \tag{5}$$

$$C_P = \frac{1}{T}\int_t^{t+T}\int_S C_p(\mathbf{V}\cdot \mathrm{d}\mathbf{A})\, \mathrm{d}t \tag{6}$$

$$\eta = \frac{C_t U_\infty}{C_P} \tag{7}$$

The power coefficient C_P accounts for the rate of average work required to maintain the flapping motion. It should be noted that the mass, and therefore the inertia, of the airfoil is ignored in the evaluation of the power coefficient. Note that $\beta = 0$ sets the objective function to the normalized thrust coefficient.

A gradient-based optimization process is employed. The gradient vector of the objective function ∇O provides the direction of the steepest ascent, along which the objective function has the maximum rate of change:

$$\nabla O = \frac{\partial O}{\partial V_1}\mathbf{v}_1 + \frac{\partial O}{\partial V_2}\mathbf{v}_2 + \cdots \tag{8}$$

where V_i are the optimization variables, and the $\mathbf{v}_i$ are the corresponding unit vectors in the variable space. The components of the gradient vector are evaluated numerically by computing the objective function for a perturbation of an optimization variable one at a time. It should be noted that the evaluation of these vector components requires an unsteady flow solution over a few periods of the flapping motion until a periodic flow behavior is reached. The optimization step size, $\Delta\mathbf{S} = \varepsilon(\nabla O/|\nabla O|)$, is determined by a line search algorithm, in which ε is incremented gradually until the objective function is maximized. The optimization process continues until a local maximum in the optimization space is reached. The convergence criteria for the optimization process is the change in the objective function being less than 1% in the line search process.

D. Parallel Processing

In the solution of unsteady flows, a parallel algorithm based on domain decomposition is implemented in a master-worker paradigm. The background grid (Fig. 3) is partitioned into two overlapping subgrids at the symmetry plane. The computational domain is then decomposed into a total of four subgrids for parallel computing [23,24]. The holes in the background grid formed by the overset airfoil grids are excluded from the computations by an *i-blanking* algorithm. The conservative flow variables are interpolated at the intergrid boundaries formed by the overset grids [23] at each time step of the unsteady solution. Also, the flow variables at the overlapping boundary of the subgrids decomposed from the background grid are exchanged among the corresponding processes at each time step. `PVM` (version 3.4.5) library routines are used for interprocess communication. In the optimization process, the components of the gradient vector that require unsteady flow solutions with perturbed optimization variables are also computed in parallel. Computations are performed in a cluster of Linux-based computers with dual Xeon and Pentium-D processors.

III. Results and Discussion

In this study, the optimization studies are performed for a range of flapping frequencies and flow Reynolds numbers at a fixed mean distance between airfoils, $y_0 = 1.4c$. The overset grid system is formed by two 231×36 size airfoil grids and a 135×260 size background grid. The optimization variables are taken as the plunge and pitch amplitudes and the phase angle between them. The optimum values obtained are compared with those of a single flapping airfoil. The computed unsteady flow solutions are analyzed in terms of the periodic variation of the aerodynamic loads, the effective angle of attack, and the unsteady particle traces. The low-speed, laminar flows are computed at a Mach number of $M = 0.1$.

Table 1 summarizes the optimization cases studied. The optimization variables are denoted by V in the table. The optimization of the flapping motion parameters for a single flapping airfoil is also performed at the optimum plunge amplitude obtained in the biplane configuration for the first three cases. Flows at $Re = 5000$, 10,000, and 20,000 are considered to assess the effect of Reynolds number on the optimization parameters. The evaluation of each gradient vector component requires about 3–6 periods of unsteady flow solution. A typical optimization process takes about 15–25 clock hours in a parallel computing environment with 12 2 GHz Pentium-4 processors.

In cases 1–9, where $\beta = 0.0$, the thrust is maximized. The initial conditions for the optimization variables are taken as the optimum values obtained in the earlier optimization study with nondeforming grids [20]. In the remaining three cases, a linear combination of thrust and efficiency is maximized with $\beta = 0.5$. The optimization results for all the cases are given in Table 2.

The optimization steps for case 1, where $Re = 10,000$, are given in Fig. 4. As the optimization variables change along the optimization steps, the thrust increases. The maximum thrust coefficient of $C_t = 0.21$ is reached at $h_0 = 0.54$, $\alpha_0 = 10.4$ deg and $\phi = 79.9$ deg, for which the propulsive efficiency turns out to be $\eta = 46.5\%$. In the previous study [20] with a limited plunge amplitude of $h_{0_{\max}} = 0.4$, the corresponding optimum values were $\alpha_0 = 6.5$ deg, $\phi = 76.5$ deg, $C_t = 0.12$, and $\eta = 46.0\%$. The study shows that, once the limitation on plunge amplitude is removed, the optimum plunge amplitude increases, and a significantly higher thrust is produced. On the other hand, for a single flapping airfoil at $h_0 = 0.54$, the optimization of α_0 and ϕ variables results in a maximum thrust of $C_t = 0.17$ with a propulsive efficiency of $\eta = 44.8\%$. It shows that, for this case, the biplane configuration produces more thrust per airfoil.

The periodic variation of the effective angle of attack and the unsteady drag for both the dual and the single flapping airfoils are compared in Fig. 5. The corresponding flapping motions and the unsteady flowfields are given in Figs. 6 and 7, respectively. It is observed that the leading-edge vortices generated during the upstroke and the downstroke of the flapping airfoils grow stronger in the case of the biplane configuration. In addition, the vortical structures and the separated flow regions over the airfoil surface are not symmetric during the upstroke and the downstroke in the biplane configuration. The separated flow at the trailing edge is larger when

Table 1 Optimization cases

Case	β	Re	k	h_0	α_0, deg	ϕ, deg
1	0.0	10,000	1.0	V	V	V
2	0.0	10,000	1.5	V	V	V
3	0.0	10,000	2.0	V	V	V
4	0.0	5000	1.0	V	V	V
5	0.0	5000	1.5	V	V	V
6	0.0	5000	2.0	V	V	V
7	0.0	20,000	1.0	V	V	V
8	0.0	20,000	1.5	V	V	V
9	0.0	20,000	2.0	V	V	V
10	0.5	10,000	1.0	V	V	V
11	0.5	10,000	1.5	V	V	V
12	0.5	10,000	2.0	V	V	V

Table 2 Optimization results

Case				Airfoils in biplane configuration					Single airfoil				
	β	k	Re	h_0	α_0, deg	ϕ, deg	C_t	η, %	h_0	α_0, deg	ϕ, deg	C_t	η, %
1	0.0	1.0	10,000	0.54	10.4	79.9	**0.21**	47	0.54	9.93	84.3	**0.17**	45
2	0.0	1.5	10,000	0.53	11.6	93.7	**0.45**	41	0.53	15.8	112.	**0.38**	45
3	0.0	2.0	10,000	0.47	2.32	39.0	**0.38**	16	0.47	20.4	123.	**0.56**	42
4	0.0	1.0	5000	0.52	10.1	79.3	**0.19**	46	——	——	——	——	——
5	0.0	1.5	5000	0.56	11.6	92.9	**0.49**	39	——	——	——	——	——
6	0.0	2.0	5000	0.48	0.58	37.2	**0.36**	14	——	——	——	——	——
7	0.0	1.0	20,000	0.53	6.16	84.7	**0.21**	40	——	——	——	——	——
8	0.0	1.5	20,000	0.54	10.7	92.8	**0.50**	41	——	——	——	——	——
9	0.0	2.0	20,000	0.48	6.11	38.1	**0.38**	17	——	——	——	——	——
10	0.5	1.0	10,000	0.46	10.9	78.7	**0.15**	**52**	——	——	——	——	——
11	0.5	1.5	10,000	0.51	12.9	92.6	**0.39**	**45**	——	——	——	——	——
12	0.5	2.0	10,000	0.43	6.06	38.9	**0.31**	**19**	——	——	——	——	——

the airfoils move apart from each other, and the leading-edge vortex formed is not as strong as the one formed when the airfoils come close together.

It is observed that, although the α_0 and the ϕ values do not differ significantly in both cases, the biplane configuration produces about 25% more thrust. The periodic variation of thrust given in Fig. 5 shows that the biplane configuration produces higher thrust at about the midplunge position of the airfoils, $h_0 = 0.0 \uparrow$ and $h_0 = 0.0 \downarrow$. The higher thrust at $h_0 = 0.0 \uparrow$ is attributed to the leading-edge vortex formed earlier than it is in the case of the single airfoil. Whereas, as the airfoils approach each other at about $h_0 = 0.0 \downarrow$, the induced jetlike flow between the airfoils appears to be responsible for the higher thrust generation.

The higher frequency flapping motions optimized for the maximum thrust at $k = 1.5$ and $k = 2.0$, and the corresponding unsteady flowfields, are given in Figs. 8–11. At $k = 1.5$, the biplane configuration still produces higher average thrust per airfoil than the single flapping airfoil (Fig. 12). The time lines formed by the particle traces (Figs. 7, 9, and 11) again reveal a jetlike flow between the airfoils as the airfoils approach each other. It appears that the jetlike flow similarly augments the thrust generation.

On the other hand, at $k = 2.0$, the maximum thrust produced by the biplane configuration drops significantly as compared with the single airfoil case (Figs. 13 and 14). In the biplane configurations, it is observed that, as the airfoils come closer at the symmetry plane, they tend to align with the freestream, and the instantaneous pitch angle α goes to zero. Such an alignment is needed to keep the flow between

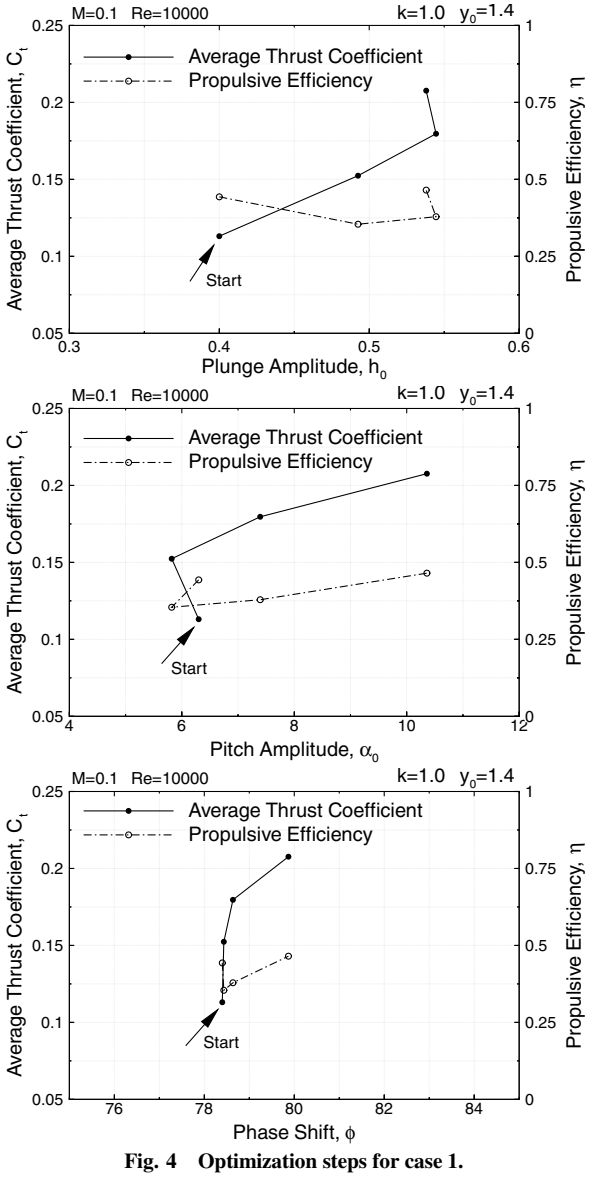

Fig. 4 Optimization steps for case 1.

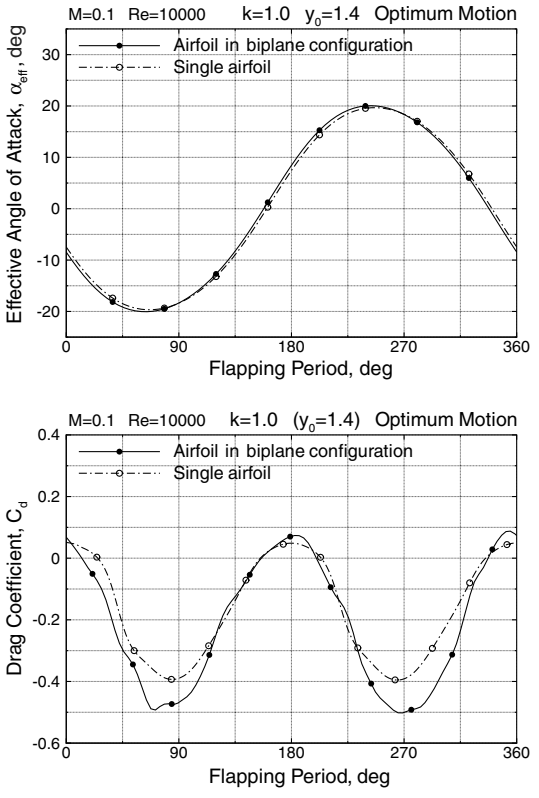

Fig. 5 Variation of the effective angle of attack and drag coefficient for case 1.

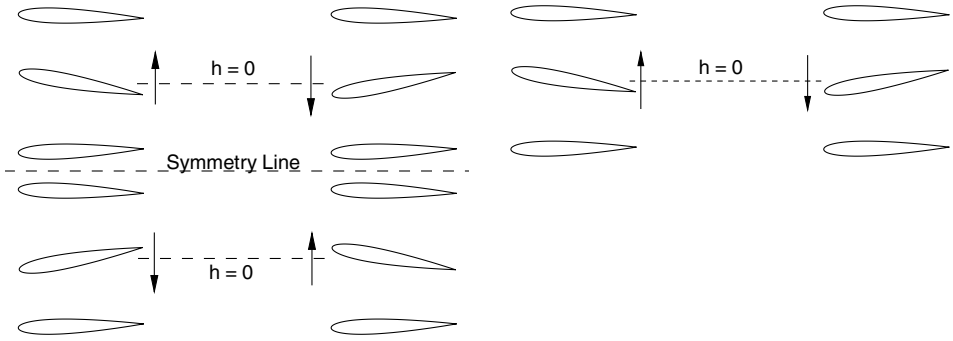

Fig. 6 Optimum motion for case 1.

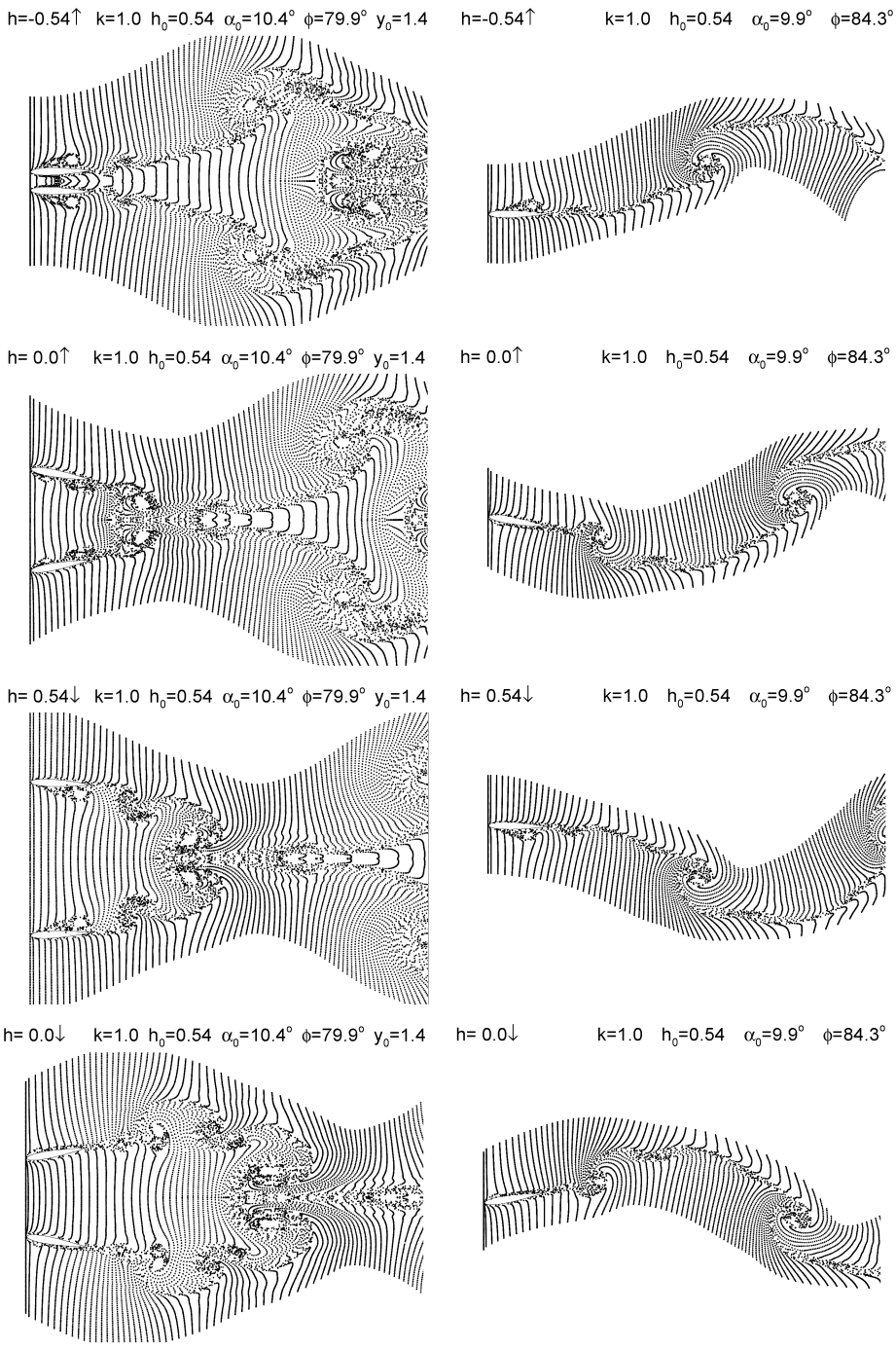

Fig. 7 Particle traces for case 1.

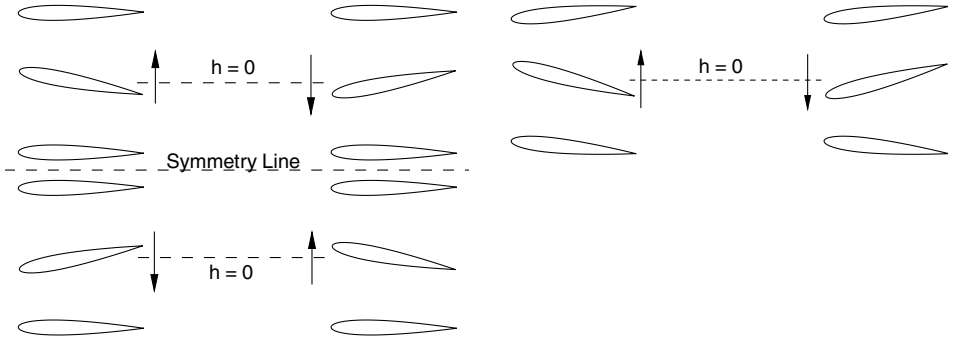

Fig. 8 Optimum motion for case 2.

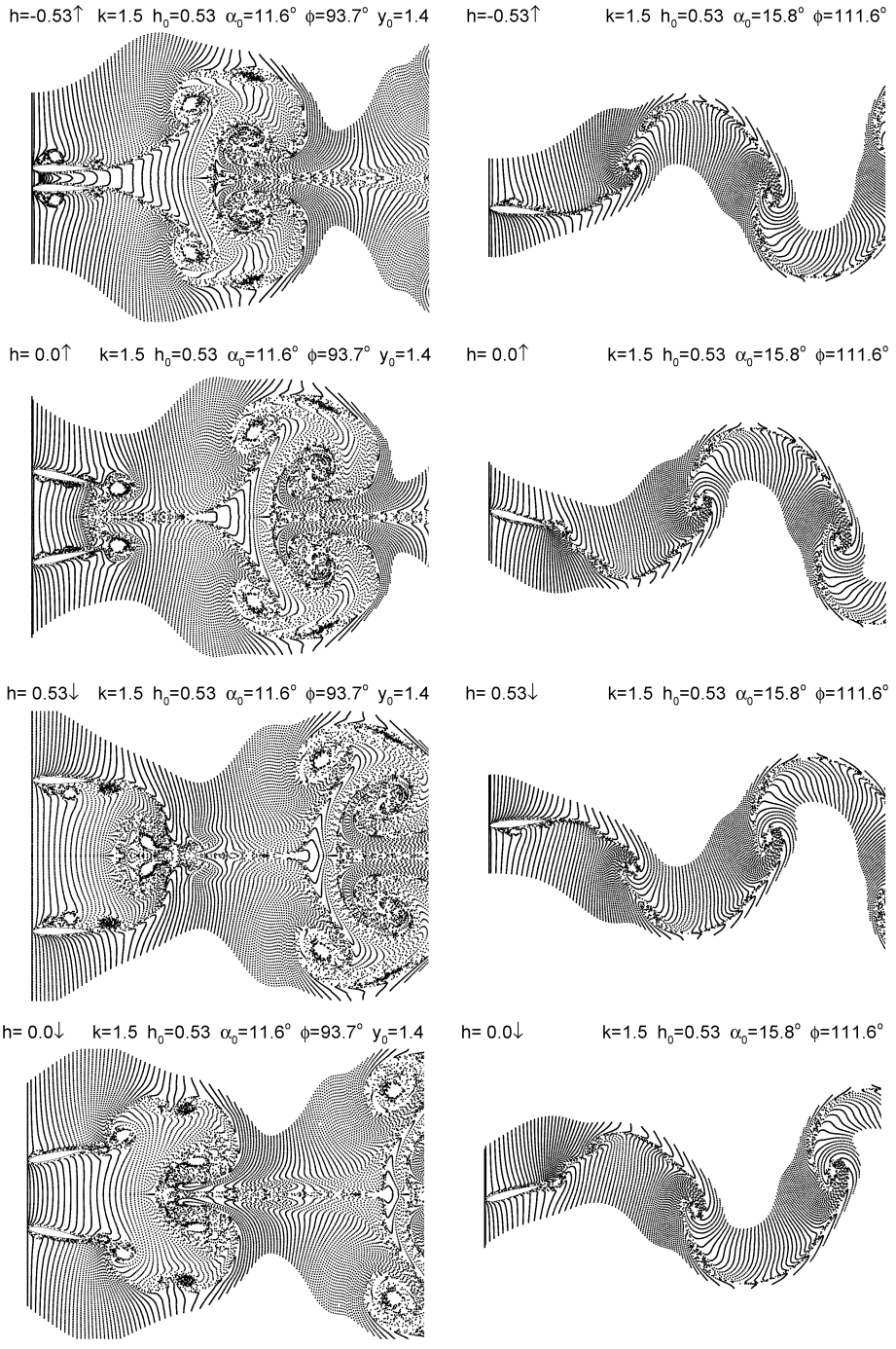

Fig. 9 Particle traces for case 2.

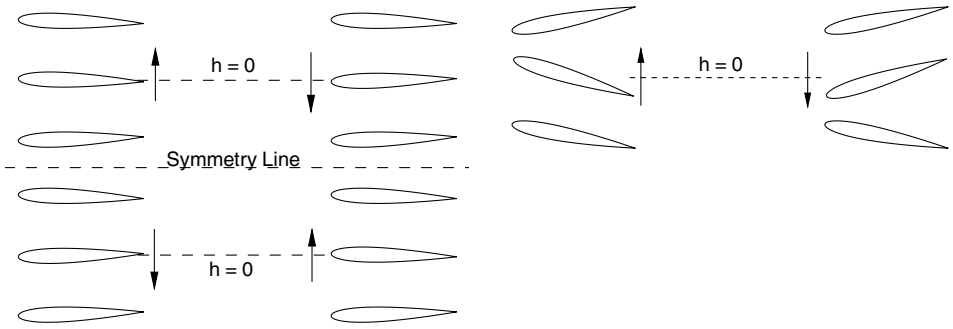

Fig. 10 Optimum motion for case 3.

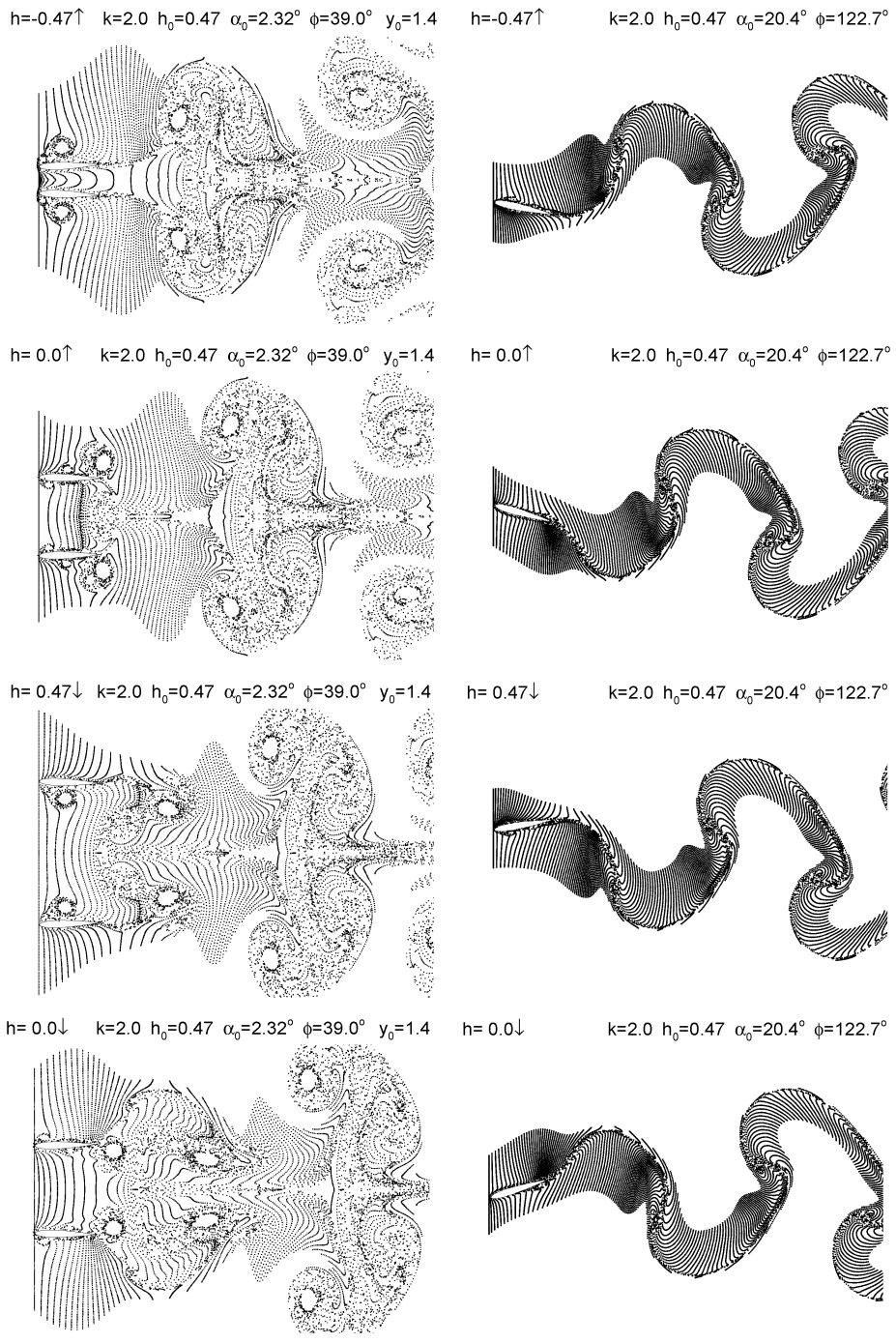

Fig. 11 Particle traces for case 3.

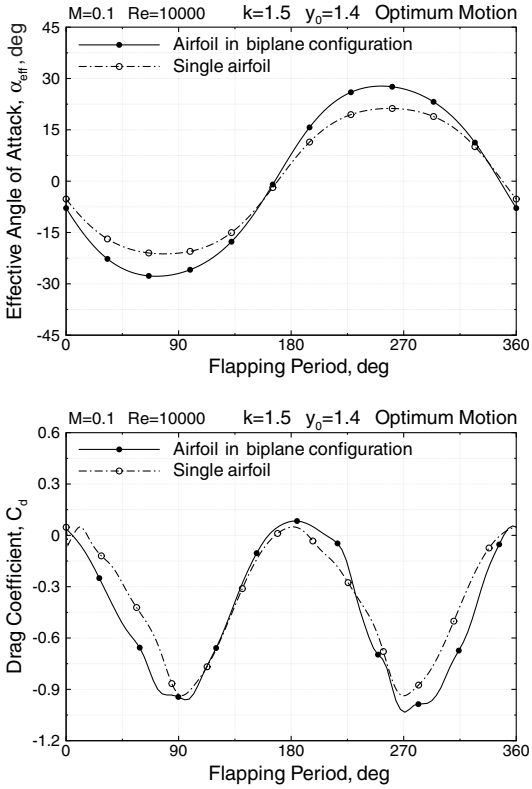

Fig. 12 Variation of the effective angle of attack and drag coefficient for case 2.

airfoils mostly attached, and consequently not to increase the drag significantly. In case 3, with $k = 2.0$, the pitch amplitude reduces to $\alpha_0 = 2.32$ deg, and the airfoils tend to flap predominantly in plunge, which is in contrast to the increasing pitch amplitude with flapping

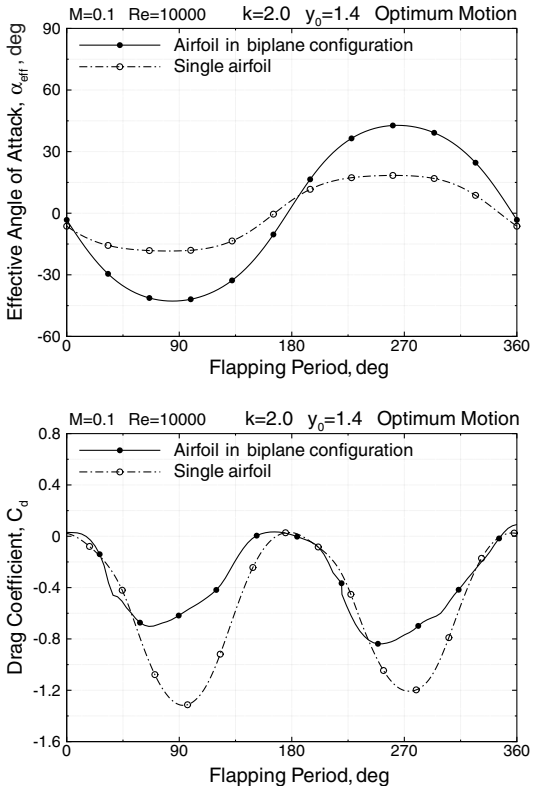

Fig. 13 Variation of the effective angle of attack and drag coefficient for case 3.

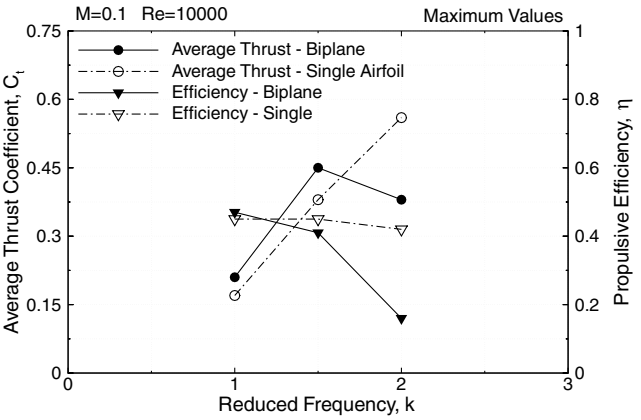

Fig. 14 Maximum thrust values and propulsive efficiencies.

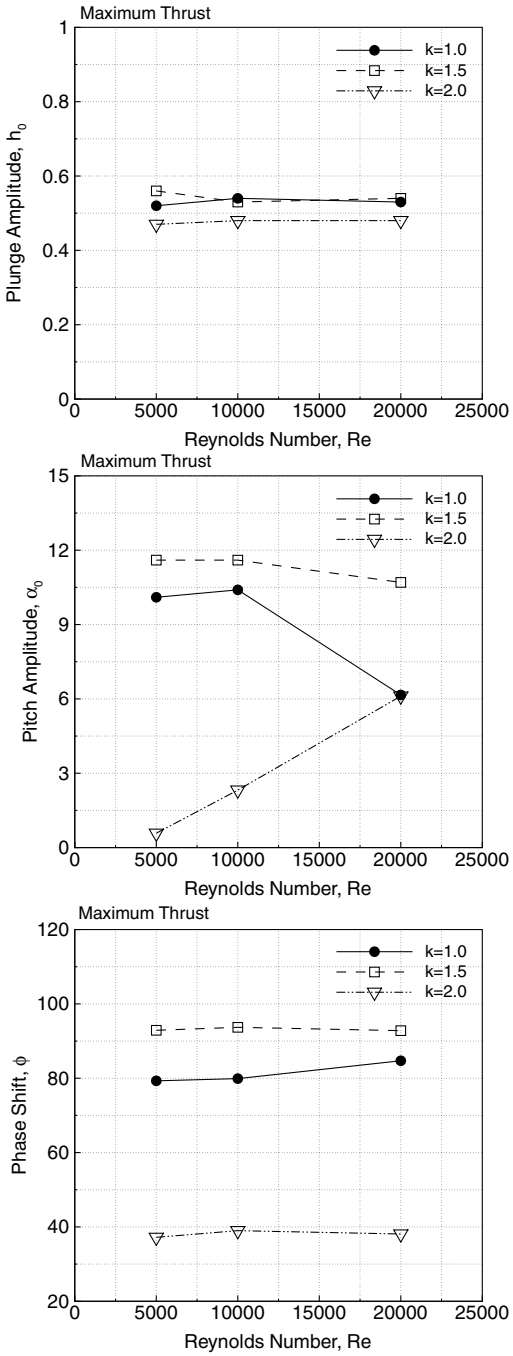

Fig. 15 Influence of Reynolds number on the optimum flapping parameters.

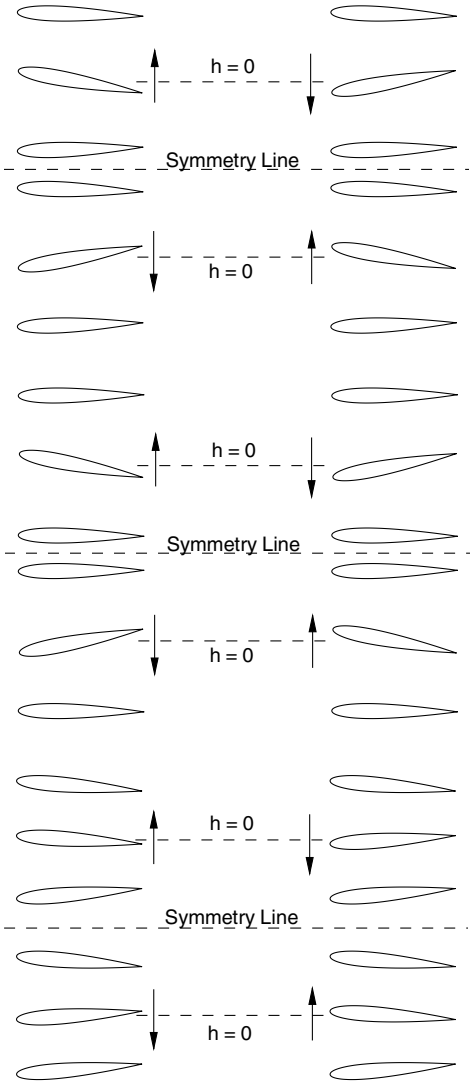

Fig. 16 Optimum motions.

frequency in the single airfoil case. In addition, the airfoils stay at large effective angle of attacks for a longer duration (Fig. 13), which promotes the formation of a leading-edge vortex. As shown in Fig. 11, the presence of strong leading-edge vortices reduces the propulsive efficiency significantly. It is apparent that, at high frequencies, the flapping airfoils in a biplane configuration do not produce as much thrust as a single flapping airfoil, and they are not as efficient either.

The optimization cases 1–3, which are performed at $Re = 10,000$, are repeated for $Re = 5000$ and $Re = 20,000$ in cases 4–9 to investigate the Reynolds number effect. Table 2 shows that the maximum thrust values at $k = 1.0$, 1.5, and 2.0 do not vary significantly with Reynolds number. The corresponding optimum flapping parameters are shown in Fig. 15. The optimum flapping motions have almost a fixed plunge amplitude h_0 and a phase shift ϕ. However, the optimum pitch amplitude α_0 varies significantly with the Reynolds numbers.

The objective function for the optimization cases 10, 11, and 12 is taken as an equally weighted combination of thrust and propulsive efficiency with $\beta = 0.5$. The optimum motions obtained for these cases now result in higher efficiencies than the previous cases at the same flapping frequencies. Figure 16 shows the optimum flapping motions for cases 10, 11, and 12, respectively. In cases 3 and 12, where $k = 2.0$, the optimum flapping motions are not quite similar, yet they almost produce the same thrust. Figure 17 shows the particle traces for case 11, where the flowfield is quite similar to that of case 2. It is observed that, for an improved efficiency, the optimum pitch amplitude increases from 11.6 to 12.9 deg, which reduces the effective angle of attack and delays the vortex formation at the leading edge. Higher propulsive efficiencies are achieved at the expense of slightly reduced thrust values.

It has been noted in previous studies [25,26] that optimum flapping–wing flight conditions seem to occur within a narrow band of Strouhal number, defined as $S_r = (k/2\pi)A$, where A is the total excursion of the trailing edge. It should be noted that, in the cases studied, the incidence angle (pitch position) is almost zero at the peak plunge positions, and the excursion of the trailing edge is equal to the peak-to-peak plunge amplitude $2h_0$. Using the preceding definition, and taking the peak-to-peak plunge amplitude as the total excursion of the trailing edge, the optimal conditions displayed in Table 2 all occur in the Strouhal number range between 0.15 and 0.3, which are

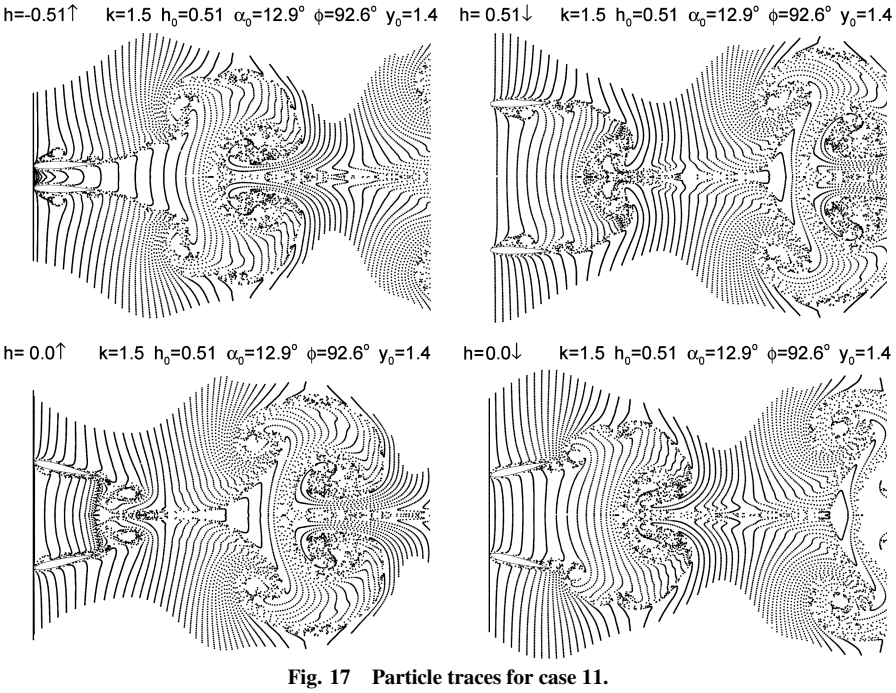

Fig. 17 Particle traces for case 11.

in agreement with the findings of Taylor et al. [25] and Young and Lai [26].

IV. Conclusions

A gradient-based optimization of flapping motion parameters is successfully applied to maximize the thrust and/or the propulsive efficiency of flapping airfoils in a biplane configuration at a range of flapping frequencies and Reynolds numbers. The flapping motion is defined by combined plunging and pitching motions. The plunge and the pitch amplitudes, and the phase angle between them, are taken as the optimization variables. The computations show that, in the Strouhal number range $0.17 < Sr < 0.25$, the flapping airfoils in a biplane configuration produce as much as 25% more thrust per airfoil than a single flapping airfoil. However, at a Strouhal number of $Sr = 0.30$, the maximum thrust production and the propulsive efficiency diminishes significantly, which is attributed to the constrained pitching motion in the biplane configuration.

References

[1] Mueller, T. J. (ed.), *Fixed and Flapping Wing Aerodynamics for Micro Air Vehicles*, Vol. 195, Progress in Aeronautics and Astronautics, AIAA, Reston, VA, 2001.

[2] Shyy, W., Berg, M., and Lyungvist, D., "Flapping and Flexible Wings for Biological and Micro Air Vehicles," Vol. 35, Progress in Aerospace Sciences, Pergamon, New York, 1999, pp. 455–505.

[3] Lai, J. C. S., and Platzer, M. F., "The Jet Characteristics of a Plunging Airfoil," *AIAA Journal*, Vol. 37, No. 12, Dec. 1999, pp. 1529–1537. doi:10.2514/2.641

[4] Jones, K. D., Dohring, C. M., and Platzer, M. F., "An Experimental and Computational Investigation of the Knoller-Beltz Effect," *AIAA Journal*, Vol. 36, No. 7, 1998, pp. 1240–1246. doi:10.2514/2.505

[5] Anderson, J. M., Streitlen, K., Barrett, D. S., and Triantafyllou, M. S., "Oscillating Foils of High Propulsive Efficiency," *Journal of Fluid Mechanics*, Vol. 360, 1998, pp. 41–72. doi:10.1017/S0022112097008392

[6] Schouveiler, L., Hover, F. S., and Triantafyllou, M. S., "Performance of Flapping Foil Propulsion," *Journal of Fluids and Structures*, Vol. 20, No. 7, Special Issue, Oct. 2005, pp. 949–959. doi:10.1016/j.jfluidstructs.2005.05.009

[7] Lewin, G. C., and Haj-Hariri, H., "Modelling Thrust Generation of a Two-Dimensional Heaving Airfoil in a Viscous Flow," *Journal of Fluid Mechanics*, Vol. 492, Oct. 2003, pp. 339–362. doi:10.1017/S0022112003005743

[8] Hover, F. S., Haugsdal, Ø., and Triantafyllou, M. S., "Effect of Angle of Attack Profiles in Flapping Foil Propulsion," *Journal of Fluids and Structures*, Vol. 19, No. 1, 2004, pp. 37–47. doi:10.1016/j.jfluidstructs.2003.10.003

[9] Lee, J.-S., Kim, C., and Kim, K. H., "Design of Flapping Airfoil for Optimal Aerodynamic Performance in Low-Reynolds Number Flows," *AIAA Journal*, Vol. 44, No. 9, 2006, pp. 1960–1972. doi:10.2514/1.15981

[10] Tuncer, I. H., and Platzer, M. F., "Computational Study of Flapping Airfoil Aerodynamics," *Journal of Aircraft*, Vol. 37, No. 3, 2000, pp. 514–520. doi:10.2514/2.2628

[11] Tuncer, I. H., Lai, J., Ortiz, M. A., and Platzer, M. F., "Unsteady Aerodynamics of Stationary/Flapping Airfoil Combination in Tandem," AIAA Paper No. 97-0659, 1997.

[12] Tuncer, I. H., and Platzer, M. F., "Thrust Generation Due to Airfoil Flapping," *AIAA Journal*, Vol. 34, No. 2, 1996, pp. 324–331. doi:10.2514/3.13067

[13] Isogai, K., Shinmoto, Y., and Watanabe, Y., "Effects of Dynamic Stall on Propulsive Efficiency and Thrust of a Flapping Airfoil," *AIAA Journal*, Vol. 37, No. 10, 1999, pp. 1145–1151. doi:10.2514/2.589

[14] Young, J., and Lai, J. C. S., "Oscillation Frequency and Amplitude Effects on the Wake of a Plunging Airfoil," *AIAA Journal*, Vol. 42, No. 10, 2004, pp. 2042–2052. doi:10.2514/1.5070

[15] Jones, K. D., Bradshaw, C. J., Papadopoulos, J., and Platzer, M. F., "Bio-Inspired Design of Flapping-Wing Micro Air Vehicles," *Aeronautical Journal*, Vol. 109, No. 1098, Aug. 2005, pp. 385–393.

[16] Jones, K. D., and Platzer, M. F., "Experimental Investigation of the Aerodynamic Characteristics of Flapping-Wing Micro Air Vehicles," AIAA Paper No. 2003-0418, Jan. 2003.

[17] Jones, K. D., Duggan, S. J., and Platzer, M. F., "Flapping-Wing Propulsion for a Micro Air Vehicle," *39th Aerospace Sciences Meeting and Exhibit*, AIAA Paper No. 2001-126, Jan. 2001.

[18] Jones, K. D., Castro, B. M., Mahmoud, O., Pollard, S. J., Platzer, M. F., Neef, M. F., Gonet, K., and Hummel, D., "A Collaborative Numerical and Experimental Investigation of Flapping-Wing Propulsion," AIAA Paper No. 2002-0706, Jan. 2002.

[19] Platzer, M. F., and Jones, K. D., "The Unsteady Aerodynamics of Flapping-Foil Propellers," *Proceedings of the 9th International Symposium on Unsteady Aerodynamics, Aeroacoustics and Aeroelasticity of Turbomachines*, Presses Univ. de Grenoble, Lyon, France, 2000, pp. 123–147.

[20] Kaya, M., and Tuncer, I. H., "Parallel Optimization of Flapping Airfoils in a Biplane Configuration for Maximum Thrust," *Proceedings of Parallel CFD 2004 Conference*, Elsevier, Amsterdam, July 2005, pp. 137–144.

[21] Tuncer, I. H., and Kaya, M., "Optimization of Flapping Airfoils For Maximum Thrust and Propulsive Efficiency," *AIAA Journal*, Vol. 43, Nov. 2005, pp. 2329–2341. doi:10.2514/1.816

[22] Tuncer, I. H., and Kaya, M., "Thrust Generation Caused by Flapping Airfoils in a Biplane Configuration," *Journal of Aircraft*, Vol. 40, No. 3, May–June 2003, pp. 509–515. doi:10.2514/2.3124

[23] Tuncer, I. H., "A 2-D Unsteady Navier–Stokes Solution Method with Moving Overset Grids," *AIAA Journal*, Vol. 35, March 1997, pp. 471–476. doi:10.2514/2.153

[24] Tuncer, I. H., and Kaya, M., "Parallel Computation of Flows Around Flapping Airfoils in Biplane Configuration," *Proceedings of Parallel CFD 2002 Conference*, Elsevier, Amsterdam, April 2003, pp. 523–530.

[25] Taylor, G. K., Nudds, R. L., and Thomas, A. L. R., "Flying and Swimming Animals Cruise at a Strouhal Number Tuned for High Power Efficiency," *Nature (London)*, Vol. 425, Oct. 2003, pp. 707–711. doi:10.1038/nature02000

[26] Young, J., and Lai, J. C. S., "Mechanisms Influencing the Efficiency of Oscillating Airfoil Propulsion," *AIAA Journal*, Vol. 45, No. 7, July 2007, pp. 1695–1702. doi:10.2514/1.27628